

Enhancing entanglement and steering in a hybrid atom-optomechanical system via Duffing nonlinearity

Ling-Hui Dong(董凌晖), Xiao-Jie Wu(武晓捷), Cheng-Hua Bai(白成华), and Shao-Xiong Wu(武少雄)

Citation: Chin. Phys. B, 2025, 34 (**2**): 020304. DOI: 10.1088/1674-1056/ad9ba2
Journal homepage: http://cpb.iphy.ac.cn; http://iopscience.iop.org/cpb

What follows is a list of articles you may be interested in

Established conversions for hybrid entangled states assisted by error-predicted parity-discriminated devices

Fang-Fang Du(杜芳芳), Zhi-Guo Fan(范志国), Xue-Mei Ren(任雪梅), Ming Ma(马明), and Wen-Yao Liu(刘文耀)
Chin. Phys. B, 2025, 34 (**1**): 010303. DOI: 10.1088/1674-1056/ad8fa0

Generation of macroscopic entanglement in ensemble systems based on silicon vacancy centers

Jian-Zhuang Wu(武建壮), Ying Xi(奚滢), Bo-Ya Li(李博雅), Lian-E Lu(芦连娥), and Yong-Hong Ma(马永红)
Chin. Phys. B, 2024, 33 (**9**): 090308. DOI: 10.1088/1674-1056/ad5d93

Delayed-measurement one-way quantum computing on cloud quantum computer

Zhi-Peng Yang(杨智鹏), Yu-Ran Zhang(张煜然), Fu-Li Li(李福利), and Heng Fan(范桁)
Chin. Phys. B, 2024, 33 (**9**): 090304. DOI: 10.1088/1674-1056/ad6253

Detecting the quantum phase transition from the perspective of quantum information in the Aubry-André model

Geng-Biao Wei(韦庚彪), Liu Ye(叶柳), and Dong Wang(王栋)
Chin. Phys. B, 2024, 33 (**7**): 070301. DOI: 10.1088/1674-1056/ad2f1f

Quantum circuit-based proxy blind signatures: A novel approach and experimental evaluation on the IBM quantum cloud platform

Xiaoping Lou(娄小平), Huiru Zan(咎慧茹), and Xuejiao Xu(徐雪娇)
Chin. Phys. B, 2024, 33 (**5**): 050307. DOI: 10.1088/1674-1056/ad22d5

Enhancing entanglement and steering in a hybrid atom–optomechanical system via Duffing nonlinearity

Ling-Hui Dong(董凌晖), Xiao-Jie Wu(武晓捷), Cheng-Hua Bai(白成华), and Shao-Xiong Wu(武少雄)[†]

School of Semiconductor and Physics, North University of China, Taiyuan 030051, *China*

(Received 14 September 2024; revised manuscript received 31 October 2024; accepted manuscript online 9 December 2024)

We introduce a novel scheme for achieving quantum entanglement and Einstein–Podolsky–Rosen (EPR) steering between an atomic ensemble and a mechanical oscillator within a hybrid atom–optomechanical system. The system comprises an optical cavity, a two-level atomic ensemble and a mechanical resonator that possesses Duffing nonlinearity. The interaction between these components is mediated by the cavity mode, which is driven by an external laser. Our findings indicate that optimizing the coupling strengths between photons and phonons, as well as between atoms and the cavity, leads to maximal entanglement and EPR steering. The amplitude of the driving laser plays a pivotal role in enhancing the coupling between photons and phonons, and the system maintains robust entanglement and EPR steering even under high dissipation, thereby mitigating the constraints on initial conditions and parameter precision. Remarkably, the Duffing nonlinearity enhances the system's resistance to thermal noise, ensuring its stability and entanglement protection. Our analysis of EPR steering conditions reveals that the party with lower dissipation exhibits superior stability and a propensity to steer the party with higher dissipation. These discoveries offer novel perspectives for advancing quantum information processing and communication technologies.

Keywords: quantum entanglement, EPR steering, optomechanical system, Duffing nonlinearity

PACS: 03.65.Ud, 03.67.Mn, 42.50.–p

DOI: 10.1088/1674-1056/ad9ba2 **CSTR:** 32038.14.CPB.ad9ba2

1. Introduction

In recent years, significant progress has been made in research into and application of quantum information technology, owing to the rapid development of quantum hardware. The core of these technologies lies in quantum entanglement and steering, which offer the potential for computational power that surpasses traditional computers, secure information transmission and precise measurements.[1] Quantum entanglement is a non-classical correlation that occurs where a change in the system of one quantum system results in a corresponding change in the state of another system, even when there is no direct exchange of matter or energy between them.[2–6] This characteristic not only serves as the foundation of quantum information science but also constitutes a crucial resource for quantum computing and quantum communication.

The realization of quantum entanglement relies heavily on the delicate manipulation of quantum states, and the cavity optomechanical system, known for its exceptional precision and controllability, has emerged as a unique and versatile platform for studying quantum entanglement.[7–9] This system integrates an optical cavity and a mechanical resonator, harnessing the interaction between light and the mechanical resonator to achieve precise control and measurement of quantum states, thereby demonstrating remarkable performance in the study of quantum effects, such as optomechanically induced transparency,[10–15] macroscopic quantum manipulation,[16–18] squeezed state preparation,[19–22] quantum synchronization[23] and ground-state cooling.[24–28] In cavity optomechanical systems, researchers have successfully prepared and observed quantum entanglement and Einstein–Podolsky–Rosen (EPR) steering through precise control of phase,[29] feedback control,[30–32] parametric amplification,[33–37] multi-cavity coupling[38–45] and nonlinear effects.[46–49]

In a hybrid atom–optomechanical system, the interaction between atoms and photons induces changes in the photon number distribution of the optical cavity, subsequently influencing the nonlinear coupling between the optical field, mechanical resonator and atoms.[50] This has significant implications for the study of quantum effects, such as mechanical squeezing[51] and photon blockade.[52–54] By manipulating this nonlinear coupling, we can more easily achieve the preparation and manipulation of quantum states, which can significantly enhance the effects of quantum entanglement and steering. However, despite the numerous advantages offered by the hybrid atom–optomechanical system for the investigation of quantum entanglement and steering, we still face a challenge in real experimental environments, namely, the inevitable interference from environmental factors, such as thermal noise, which can lead to decoherence and the destruction of entangled states.

Introducing Duffing nonlinearity offers an effective strat-

[†]Corresponding author. E-mail: sxwu@nuc.edu.cn

© 2025 Chinese Physical Society and IOP Publishing Ltd. All rights, including for text and data mining, AI training, and similar technologies, are reserved.

egy for the optomechanical system to resist thermal noise and enhance quantum effects. Research indicates that this nonlinearity can achieve more than 3 dB of mechanical squeezing in the highly unresolved sideband regime and exhibits robust resistance to thermal noise.[55] Combining Duffing nonlinearity with frequency modulation,[56] or introducing it alongside intracavity squeezed light in a dual-cavity optomechanical system,[57] can effectively enhance mechanical squeezing. Prior research has shown that incorporating Duffing nonlinearity can yield a significant enhancement in the squeezing of mechanical oscillators.

Inspired by the aforementioned works, in this paper we investigate quantum entanglement and EPR steering between an atomic ensemble and a mechanical oscillator within a hybrid atom–optomechanical system. We are the first to introduce the Duffing nonlinearity of a mechanical resonator into the investigation of entanglement and steering within hybrid atom–optomechanical systems. The Duffing nonlinearity not only alters but also strengthens the internal coupling strength, leading to enhanced quantum entanglement and EPR steering. What's more, the Duffing nonlinearity can enhance the resistance of the system to environmental noise.

In this paper, we first explore how varying the coupling strengths of photon–phonon and collective atom–cavity interactions influences the entanglement and EPR steering. Utilizing the Bogoliubov transformation, we identify the optimal conditions for maximizing the entanglement and steering by fine-tuning these coupling strengths. Notably, adjusting the external driving laser is pivotal for enhancing photon–phonon coupling. Furthermore, our results show that Duffing nonlinearity significantly enhances the system's resilience to thermal noise, thereby ensuring its stability and entanglement protection. Lastly, by examining the relationship between steering and the dissipation of the two modes, we conclude that the steering predominantly occurs from the mode with lower dissipation to the mode with higher dissipation. Our findings underscore the potential of this system in advancing quantum information processing applications.

The structure of this paper is as follows. In Section 2, we introduce the hybrid atom–optomechanical model and derive the effective Hamiltonian by using the techniques of frame rotation and standard linearization. In Section 3, we investigate quantum entanglement and steering between the atomic ensemble and the mechanical resonator, exploring the impact of different coupling strengths. We demonstrate that Duffing nonlinearity plays a crucial role in enhancing the robustness of the system to thermal noise, and discuss the factors influencing the direction of steering. Section 4 presents our conclusions.

2. Theoretical model

We consider a hybrid atom–optomechanical system as schematically depicted in Fig. 1, consisting of a cavity, a mechanical resonator and a two-level atomic ensemble. In the model, Duffing nonlinearity is introduced into the mechanical oscillator and the cavity field is driven by a coherent laser. The total Hamiltonian of the system is described by (in units of $\hbar = 1$)

$$\begin{aligned} H_0 &= \omega_c c^\dagger c + \omega_m b^\dagger b + \omega_a \sum_j \sigma_z^j + \frac{\eta}{2}(b^\dagger + b)^4 \\ &\quad - g_{cb} c^\dagger c (b^\dagger + b) + g_{ca}(c^\dagger \sum_j \sigma_-^j + c \sum_j \sigma_+^j) \\ &\quad + E(c^\dagger \mathrm{e}^{-\mathrm{i}\omega_d t} + c\,\mathrm{e}^{\mathrm{i}\omega_d t}), \end{aligned} \tag{1}$$

where c ($c^\dagger$) and b ($b^\dagger$) are the annihilation (creation) operators of the cavity mode and the mechanical mode and $\sigma_{+,-,z}^j$ are the Pauli matrices of the atom numbered j ($j = 1, \ldots, N$) in the atomic ensemble. These operators and matrices correspond to resonance frequencies ω_c, ω_m and ω_a, respectively. The coefficients η, g_{cb} and g_{ca} represent the Duffing nonlinearity, the photon–phonon coupling strength and the photon–atom coupling strength, respectively. The cavity is driven by a coherent laser with amplitude E and frequency ω_d.

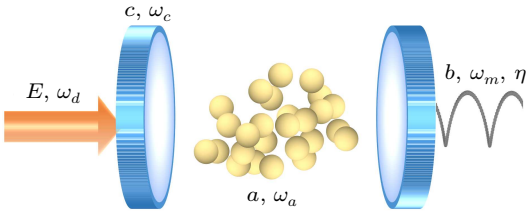


Fig. 1. Schematic diagram of the hybrid atom–optomechanical system. The system consists of a cavity, a two-level atomic ensemble and a mechanical resonator that incorporates Duffing nonlinearity. The cavity is driven by an external laser.

In order to simplify the Hamiltonian of the model, the collective behavior of the atomic ensemble can be described in terms of a collective bosonic annihilation (creation) operator, denoted as a ($a^\dagger$) in the Holstein–Primakoff representation[58]

$$\begin{aligned} \sum_j \sigma_+^j &= a^\dagger \sqrt{N - a^\dagger a} \simeq \sqrt{N} a^\dagger, \\ \sum_j \sigma_-^j &= \sqrt{N - a^\dagger a}\, a \simeq \sqrt{N} a, \\ \sum_j \sigma_z^j &= a^\dagger a - \frac{N}{2}. \end{aligned} \tag{2}$$

The Hamiltonian H_0 in Eq. (1) can be rewritten as follows:

$$\begin{aligned} H_c &= \omega_c c^\dagger c + \omega_m b^\dagger b + \omega_a a^\dagger a + \frac{\eta}{2}(b^\dagger + b)^4 \\ &\quad - g_{cb} c^\dagger c (b^\dagger + b) + G_{ca}(c^\dagger a + c a^\dagger) \\ &\quad + E(c^\dagger \mathrm{e}^{-\mathrm{i}\omega_d t} + c\,\mathrm{e}^{\mathrm{i}\omega_d t}), \end{aligned} \tag{3}$$

where $G_{ca} = g_{ca}\sqrt{N}$ represents the collective atom–cavity coupling strength. Employing the frame rotation under frequency ω_d, the Hamiltonian H_c in Eq. (3) can be expressed as

$$\begin{aligned} H_{\rm r} =& \Delta_c c^\dagger c + \omega_m b^\dagger b + \Delta_a a^\dagger a + \frac{\eta}{2}(b^\dagger + b)^4 \\ & - g_{cb} c^\dagger c (b^\dagger + b) + G_{ca}(c^\dagger a + c a^\dagger) \\ & + E(c^\dagger + c), \end{aligned} \tag{4}$$

where $\Delta_c = \omega_c - \omega_d$ and $\Delta_a = \omega_a - \omega_d$ represent the detuning of the cavity and the atomic ensemble, respectively, with respect to the driving laser.

Taking into account the effects of dissipation in the cavity, mechanical resonator, atomic ensemble and the corresponding environmental noise, the dynamics of the system can be described by the nonlinear quantum Langevin equation[59]

$$\begin{aligned} \dot{c} =& -{\rm i}\Delta_c c + {\rm i} g_{cb} c (b^\dagger + b) - {\rm i} G_{ca} a - {\rm i} E - \frac{\kappa_c}{2} c + \sqrt{\kappa_c} c_{\rm in}, \\ \dot{b} =& -{\rm i}\omega_m b - 2{\rm i}\eta (b^\dagger + b)^3 + {\rm i} g_{cb} c^\dagger c - \frac{\gamma_m}{2} b + \sqrt{\gamma_m} b_{\rm in}, \\ \dot{a} =& -{\rm i}\Delta_a a - {\rm i} G_{ca} c - \frac{\gamma_a}{2} a + \sqrt{\gamma_a} a_{\rm in}, \end{aligned} \tag{5}$$

where $\kappa_c, \gamma_m, \gamma_a$ and $c_{\rm in}, b_{\rm in}, a_{\rm in}$ are the dissipation rates and noise operators for the cavity, mechanical resonator and atomic ensemble, respectively.

By employing the standard linearization method and utilizing the displacement transformation, equation (5) can be rewritten in the form of a sum of steady-state mean values and quantum fluctuation operators, i.e., $o = \langle o \rangle + \delta o$ $(o = a, b, c)$. The differential equation for the steady-state mean part is given by

$$\begin{aligned} \langle \dot{c} \rangle =& (-{\rm i}\tilde{\Delta}_c - \frac{\kappa_c}{2})\langle c \rangle - {\rm i} G_{ca} \langle a \rangle - {\rm i} E, \\ \langle \dot{b} \rangle =& (-{\rm i}\omega_m - \frac{\gamma_m}{2})\langle b \rangle - 2{\rm i}\eta [(\langle b^\dagger \rangle + \langle b \rangle)^3 + 3(\langle b^\dagger \rangle + \langle b \rangle)] \\ & + {\rm i} g_{cb} |\langle c \rangle|^2, \\ \langle \dot{a} \rangle =& (-{\rm i}\Delta_a - \frac{\gamma_a}{2})\langle a \rangle - {\rm i} G_{ca} \langle c \rangle, \end{aligned} \tag{6}$$

where $\tilde{\Delta}_c = \Delta_c - 2 g_{cb} {\rm Re}\langle b \rangle$ represents the effective detuning of the cavity. The steady-state mean value part remains constant and does not change with time. By solving Eq. (6), the mean value of the cavity mode can be given analytically as follows:

$$\langle c \rangle = \frac{E(\Delta_a - {\rm i}\frac{\gamma_a}{2})}{G_{ca}^2 + (-{\rm i}\tilde{\Delta}_c + \frac{\kappa_c}{2})(-{\rm i}\Delta_a + \frac{\gamma_a}{2})}. \tag{7}$$

By appropriately adjusting the phase of the driving laser, the steady-state mean value $\langle c \rangle$ can be treated as a real number.

Under strong driving condition and neglecting the nonlinear term, the quantum fluctuation operator part will result in the following linearized quantum Langevin equation:

$$\begin{aligned} \delta\dot{c} =& (-{\rm i}\tilde{\Delta}_c - \frac{\kappa_c}{2})\delta c + {\rm i} G_{cb}(\delta b^\dagger + \delta b) - {\rm i} G_{ca} \delta a + \sqrt{\kappa_c} c_{\rm in}, \\ \delta\dot{b} =& (-{\rm i}\tilde{\omega}_m - \frac{\gamma_m}{2})\delta b - 2{\rm i}\Lambda \delta b^\dagger \\ & + {\rm i} G_{cb}(\delta c^\dagger + \delta c) + \sqrt{\gamma_m} b_{\rm in}, \\ \delta\dot{a} =& (-{\rm i}\Delta_a - \frac{\gamma_a}{2})\delta a - {\rm i} G_{ca} \delta c + \sqrt{\gamma_a} a_{\rm in}, \end{aligned} \tag{8}$$

where the coefficients are $\tilde{\omega}_m = \omega_m + 2\Lambda$, $\Lambda = 3\eta[(\langle b \rangle + \langle b^\dagger \rangle)^2 + 1]$ and $G_{cb} = g_{cb}\langle c \rangle$. The coefficient Λ is related to the Duffing nonlinearity.

According to Eq. (8), the effective Hamiltonian can be derived as follows:

$$\begin{aligned} H_{\rm eff} =& \tilde{\Delta}_c \delta c^\dagger \delta c + \tilde{\omega}_m \delta b^\dagger \delta b + \Delta_a \delta a^\dagger \delta a \\ & + \Lambda(\delta b^{\dagger 2} + \delta b^2) - G_{cb}(\delta c^\dagger + \delta c)(\delta b^\dagger + \delta b) \\ & + G_{ca}(\delta c \delta a^\dagger + \delta c^\dagger \delta a). \end{aligned} \tag{9}$$

Transforming into the squeezing picture using $H'_{\rm eff} = S^\dagger(r) H_{\rm eff} S(r)$ with $S(r) = \exp[r(b^2 - b^{\dagger 2})/2]$ and squeezing parameter $r = (1/4)\ln[1 + 4\Lambda/\omega_m]$, the effective Hamiltonian can be re-expressed as[55]

$$\begin{aligned} H'_{\rm eff} =& \tilde{\Delta}_c \delta c^\dagger \delta c + \omega'_m \delta b^\dagger \delta b + \Delta_a \delta a^\dagger \delta a \\ & - G'_{cb}(\delta c^\dagger + \delta c)(\delta b^\dagger + \delta b) \\ & + G_{ca}(\delta c \delta a^\dagger + \delta c^\dagger \delta a), \end{aligned} \tag{10}$$

where $\omega'_m = \omega_m \sqrt{1 + 4\Lambda/\omega_m}$ is the transformed mechanical frequency and $G'_{cb} = G_{cb}(1 + 4\Lambda/\omega_m)^{-1/4}$ is the effective optomechanical coupling strength.

Since the squeezing transformation is applied to the mechanical resonator, the noise correlation function of the mechanical resonator also needs to be transformed into the squeezing picture, which is denoted as

$$\begin{aligned} \langle b_{\rm in}(t) b_{\rm in}^\dagger(t') \rangle &= (n'_{\rm th} + 1)\delta(t - t'), \\ \langle b_{\rm in}^\dagger(t) b_{\rm in}(t') \rangle &= n'_{\rm th} \delta(t - t'), \\ \langle b_{\rm in}(t) b_{\rm in}(t') \rangle &= -m\delta(t - t'), \\ \langle b_{\rm in}^\dagger(t) b_{\rm in}^\dagger(t') \rangle &= -m\delta(t - t'), \end{aligned} \tag{11}$$

where $n'_{\rm th} = n_{\rm th}\cosh 2r + \sinh^2 r$ and $m = (2n_{\rm th} + 1)\cosh r \sinh r$, with thermal mean phonon number of the mechanical resonator $n_{\rm th} = [\exp(\hbar\omega_m/k_{\rm B}T) - 1]^{-1}$ under temperature T. The noise correlation functions for the cavity and atomic ensemble are

$$\begin{aligned} &\langle c_{\rm in}(t) c_{\rm in}^\dagger(t') \rangle = \delta(t - t'), \ \ \langle c_{\rm in}^\dagger(t) c_{\rm in}(t') \rangle = 0, \\ &\langle a_{\rm in}(t) a_{\rm in}^\dagger(t') \rangle = \delta(t - t'), \ \ \langle a_{\rm in}^\dagger(t) a_{\rm in}(t') \rangle = 0. \end{aligned} \tag{12}$$

To investigate the dynamics of the system, the dimensionless orthogonal operators $X_o = (o + o^\dagger)/\sqrt{2}, Y_o = (o - o^\dagger)/({\rm i}\sqrt{2})$ and orthogonal noise operators $X_o^{\rm in} = (o_{\rm in} + o_{\rm in}^\dagger)/\sqrt{2}$, $Y_o^{\rm in} = (o_{\rm in} - o_{\rm in}^\dagger)/({\rm i}\sqrt{2})$ are introduced.

The vector of quadrature fluctuation operators can be expressed as $\mathcal{U} = [X_c, Y_c, X_b, Y_b, X_a, Y_a]^{\mathrm{T}}$, the vector of quadrature noise operators can be expressed as $\mathcal{N} = [\sqrt{\kappa_c}X_c^{\mathrm{in}}, \sqrt{\kappa_c}Y_c^{\mathrm{in}}, \sqrt{\gamma_m}X_b^{\mathrm{in}}, \sqrt{\gamma_m}Y_b^{\mathrm{in}}, \sqrt{\gamma_a}X_a^{\mathrm{in}}, \sqrt{\gamma_a}Y_a^{\mathrm{in}}]^{\mathrm{T}}$ and the quantum Langevin equation for the system can be expressed in matrix form as

$$\dot{\mathcal{U}}(t) = \mathcal{M}\mathcal{U}(t) + \mathcal{N}(t), \tag{13}$$

where the drift matrix $\mathcal{M}$ is given by

$$\mathcal{M} = \begin{bmatrix} -\frac{\kappa_c}{2} & \tilde{\Delta}_c & 0 & 0 & 0 & G_{ca} \\ -\tilde{\Delta}_c & -\frac{\kappa_c}{2} & 2G'_{cb} & 0 & -G_{ca} & 0 \\ 0 & 0 & -\frac{\gamma_m}{2} & \omega'_m & 0 & 0 \\ 2G'_{cb} & 0 & -\omega'_m & -\frac{\gamma_m}{2} & 0 & 0 \\ 0 & G_{ca} & 0 & 0 & -\frac{\gamma_a}{2} & \Delta_a \\ -G_{ca} & 0 & 0 & 0 & -\Delta_a & -\frac{\gamma_a}{2} \end{bmatrix}. \tag{14}$$

The correlation properties of the system can be characterized by a 6×6 covariance matrix $\mathcal{V}$, whose elements can be denoted as $\mathcal{V}_{ij} = \langle \mathcal{U}_i(t)\mathcal{U}_j(t') + \mathcal{U}_j(t')\mathcal{U}_i(t)\rangle/2$. Because of the Gaussian nature of quantum noise, the system will maintain a Gaussian state when the system is in a steady state, and the covariance matrix $\mathcal{V}$ can be obtained by solving the Lyapunov equation

$$\mathcal{M}\mathcal{V} + \mathcal{V}\mathcal{M}^{\mathrm{T}} = -\mathcal{D}, \tag{15}$$

where $\mathcal{D}$ denotes the noise diffusion matrix, whose elements are defined as $\mathcal{D}_{ij} = \langle \mathcal{N}_i(t)\mathcal{N}_j(t') + \mathcal{N}_j(t')\mathcal{N}_i(t)\rangle/2$. According to the noise correlation functions (11) and (12), the noise diffusion matrix $\mathcal{D}$ can be derived as follows:

$$\begin{aligned} \mathcal{D} = \frac{1}{2}\mathrm{diag}[&\kappa_c, \kappa_c, \gamma_m(2n'_{\mathrm{th}} + 1 - 2m), \\ &\gamma_m(2n'_{\mathrm{th}} + 1 + 2m), \gamma_a, \gamma_a]. \end{aligned} \tag{16}$$

The steady-state entanglement between different modes can be analyzed by reducing a 4×4 covariance matrix from the 6×6 covariance matrix

$$\mathcal{V}_{12} = \begin{bmatrix} \mathcal{V}_1 & \mathcal{V}_{\mathrm{c}} \\ \mathcal{V}_{\mathrm{c}}^{\mathrm{T}} & \mathcal{V}_2 \end{bmatrix}, \tag{17}$$

where $\mathcal{V}_1, \mathcal{V}_2$ and $\mathcal{V}_{\mathrm{c}}$ denote the 2×2 block matrices corresponding to the two modes and their correlation part, respectively. The entanglement between two modes can be measured by logarithmic negativity[60]

$$E_{\mathrm{N}} = \max[0, -\ln 2\eta^-], \tag{18}$$

where $\eta^- = [(\Sigma - \sqrt{\Sigma^2 - 4\det\mathcal{V}_{12}})/2]^{1/2}$, $\Sigma = \det\mathcal{V}_1 + \det\mathcal{V}_2 - 2\det\mathcal{V}_{\mathrm{c}}$. Besides entanglement, EPR steering can also measure the correlation between two modes. When one mode can control the state of the other mode through localized operations in its own Hilbert space, this is known as steering. Specifically, steering from mode 1 to mode 2 is defined as[61]

$$\mathcal{G}_{1\to 2} = \max\left[0, \frac{1}{2}\ln\frac{\det\mathcal{V}_1}{4\det\mathcal{V}_{12}}\right]. \tag{19}$$

In a similar way, steering from mode 1 to mode 2 is $\mathcal{G}_{2\to 1} = \max[0, \frac{1}{2}\ln\frac{\det\mathcal{V}_2}{4\det\mathcal{V}_{12}}]$.

3. Entanglement and steering between atomic ensemble and mechanical resonator

This section is dedicated to the study of entanglement E_{ab}, steering $\mathcal{G}_{b\to a}$ and steering $\mathcal{G}_{a\to b}$ between the atomic ensemble mode δa and the mechanical resonator mode δb. There is photon–phonon interaction as well as atom–photon interaction in the effective Hamiltonian H'_{eff} (10), therefore it is plausible to speculate that there is indirect entanglement and steering between the atomic system and the mechanical resonator. In Fig. 2, we plot the entanglement E_{ab}, steering $\mathcal{G}_{b\to a}$ and steering $\mathcal{G}_{a\to b}$ between the atomic ensemble mode δa and the mechanical resonator mode δb as functions of the photon–phonon coupling strength g_{cb} (a) and the collective atom–cavity coupling strength G_{ca} (b).

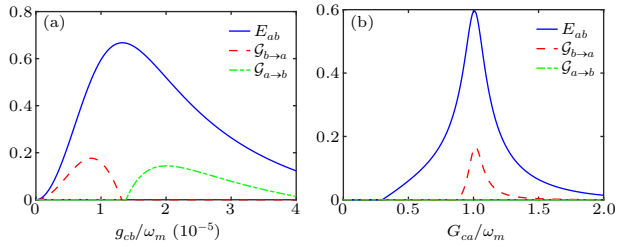


Fig. 2. The steady-state entanglement E_{ab}, steering $\mathcal{G}_{b\to a}$ and steering $\mathcal{G}_{a\to b}$ between the atomic ensemble and the mechanical resonator as functions of the photon–phonon coupling strength g_{cb}/ω_m with $G_{ca}/\omega_m = 1$ (a) and the collective atom–cavity coupling strength G_{ca} with $g_{cb}/\omega_m = 10^{-5}$ (b). The other system parameters are set as $\kappa_c/\omega_m = 0.4, \gamma_m/\omega_m = 10^{-6}, \gamma_a/\omega_m = 10^{-3}, \tilde{\Delta}_c/\omega_m = 1$, $\Delta_a/\omega_m = -1, E/\omega_m = 1.5\times 10^4$, $\Lambda/\omega_m = 0.25$ and $n_{\mathrm{th}} = 0$.

Based on the existing experimental techniques, the system parameters are set as follows: $\omega_m/2\pi = 1$ MHz, $\kappa_c/\omega_m = 0.4$, $\gamma_m/\omega_m = 10^{-6}$, $\gamma_a/\omega_m = 10^{-3}$, $\tilde{\Delta}_c/\omega_m = 1$, $\Delta_a/\omega_m = -1$ and $E/\omega_m = 1.5\times 10^4$. When the mechanical resonator is coupled to an ancillary qubit, and the coupling strength between the qubit and the mechanical resonator is much smaller than the qubit's energy level, we can introduce effective Duffing nonlinearity to the mechanical resonator. The power of the external driving laser with a wavelength of 1550 nm is $P_{\mathrm{in}} \simeq 0.4$ mW. At this power level, the backaction of the mechanical mode on the qubit is so small that it can be neglected. Therefore, the ancillary qubit can be considered as a passive system unaffected by the mechanical resonator.[55–57,62] In the subsequent analysis, we ensure the stability of the system by employing the Routh–Hurwitz criterion.[63] In addition

to this, most importantly, it is evident from Fig. 2 that both coupling strengths initially have a positive effect on enhancing the stable entanglement and steering between the atomic ensemble and the mechanical resonator. However, as the coupling strengths increase further, the values of entanglement and steering gradually decrease after each reaches its peak value.

To investigate the physical mechanism behind this result, we will delve deeper into the analysis of the interactions between the different modes of the system. In principle, the interaction part of the effective Hamiltonian $H'_{\rm eff}$ (10) can be represented by $J(\beta\delta c^\dagger + \beta^\dagger \delta c)$ with Bogoliubov mode $\beta = \delta a \cosh\lambda + \delta b^\dagger \sinh\lambda$, where $J = \sqrt{G_{ca}^2 - G_{cb}'^2}$ is the coupling strength between the cavity mode δc and the Bogoliubov mode β, and $\lambda = \operatorname{arctanh}(G'_{cb}/G_{ca})$ is the squeezing coefficient of the two-mode squeezing state. A two-mode squeezing state cannot be expressed as a product of two single-mode squeezing states, thus it is inherently a two-mode entangled state.[64,65] The squeezing of the Bogoliubov mode β naturally leads to the entanglement between modes δa and δb. Moreover, an increase in the squeezing coefficient λ has a positive impact on the squeezing of the Bogoliubov mode β. Thus, from this perspective, a larger λ may contribute to a stronger entanglement between modes δa and δb. However, a larger λ will result in a smaller effective coupling strength J, which will limit the cooling of the Bogoliubov mode through the beam-splitter interaction and subsequently constrain the maximum entanglement between modes δa and δb.

Figures 3(a) and 3(b) plot the entanglement E_{ab} and steering $\mathcal{G}_{b\to a}$ between the atomic ensemble mode δa and the mechanical resonator mode δb as functions of g_{cb} and Λ, respectively. Based on the above analysis, it is known that the squeezing coefficient λ monotonically increases with increase in the effective optomechanical coupling strength G'_{cb}, and G'_{cb} monotonically increases with the increase of the photon–phonon coupling strength g_{cb} and monotonically decreases with the increase of Λ. Therefore, it can be observed that when g_{cb} is large enough, entanglement can be generated even if Λ is zero; however, as the figures show, a smaller Λ is not always better, as maximum entanglement does not occur where the Λ is zero. This is because the squeezing of the Bogoliubov mode β is determined not only by the squeezing coefficient λ but also by the strength of the coupling J between the cavity mode δc and the Bogoliubov mode β. From this point of view, to obtain stronger entanglement it may be desirable to either increase G_{ca} or reduce G'_{cb}. Figures 3(c) and 3(d) plot the entanglement E_{ab} and steering $\mathcal{G}_{b\to a}$ as functions of G_{ca} and Λ, respectively.

As analyzed above, E_{ab} and $\mathcal{G}_{b\to a}$ gradually reach their maximum values as Λ and G_{ca} increase. However, it can be observed from Fig. 3 that the entanglement E_{ab} and steering $\mathcal{G}_{b\to a}$ do not increase indefinitely as g_{cb} or G_{ca} increase. The opposing effects of G'_{cb} and G_{ca} on the squeezing coefficient λ and the coupling strength J are evident. Specifically, an increase in G'_{cb} or a decrease in G_{ca} will lead to an increase in the squeezing coefficient λ, whereas the opposite behaviors will result in an increase in the coupling strength J. These two opposing effects enable the system to reach equilibrium and attain maximum entanglement at optimal values of G'_{cb} and G_{ca}.

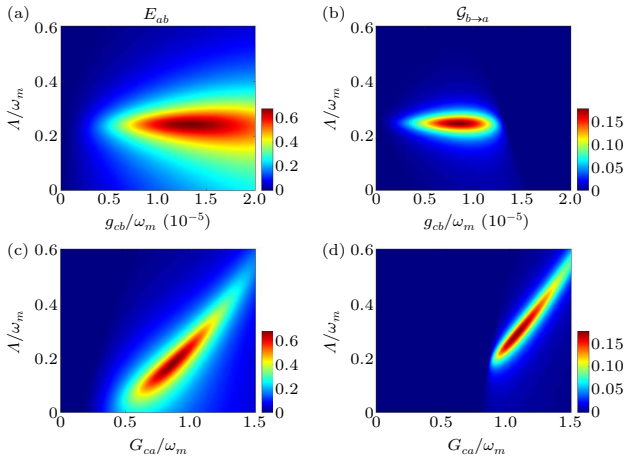


Fig. 3. (a) The steady-state entanglement E_{ab} and (b) steering $\mathcal{G}_{b\to a}$ as functions of Λ and g_{cb}. (c) The steady-state entanglement E_{ab} and (d) steering $\mathcal{G}_{b\to a}$ as functions of Λ and G_{ca}. The other parameters are the same as those in Fig. 2.

Figures 4(a) and 4(b) plot the entanglement E_{ab} and steering $\mathcal{G}_{b\to a}$ between the atomic ensemble mode δa and the mechanical resonator mode δb as functions of the photon–phonon coupling strength g_{cb} and the amplitude E of the driving laser, respectively. As g_{cb} increases, figures 4(a) and 4(b) show that the range of E that can generate entanglement and steering gradually decreases. Simultaneously, the value of E corresponding to the maximum entanglement also decreases. Similarly, as E increases, the range of g_{cb} values capable of generating entanglement along with steering gradually narrows, and the maximum entanglement corresponding to the value of g_{cb} also decreases. This phenomenon occurs because of the direct proportionality between the effective optomechanical coupling strength G'_{cb} and the product of g_{cb} and E, which implies that an optimal value of the effective optomechanical coupling strength is determined by g_{cb} and E together. Adjusting the driving amplitude E ensures that the photon–phonon coupling strength g_{cb} remains within an effective range for entanglement.

Figures 4(c) and 4(d) plot the entanglement E_{ab} and steering $\mathcal{G}_{b\to a}$ as functions of the cavity dissipation rate κ_c and the photon–phonon coupling strength g_{cb}, respectively. Because the effective optomechanical coupling strength G'_{cb} monotonically increases with increase in g_{cb} and decreases with increase in κ_c, the value of κ_c corresponding to maximum entanglement

and steering gradually increases with increasing g_{cb}. The optimal effective optomechanical coupling strength can be obtained by balancing g_{cb} and κ_c, which results in the maximum entanglement or steering. In addition, as depicted in Figs. 4(c) and 4(d), stable entanglement and steering can be achieved even with a high dissipation rate $\kappa_c/\omega_m = 5$, which may reduce the requirement for the quality factor of the cavity, consequently making it easier to implement in experiment. This has significant implications for both practical applications and research. Furthermore, a larger dissipation rate makes the system less sensitive to external noise and enhances its overall stability.

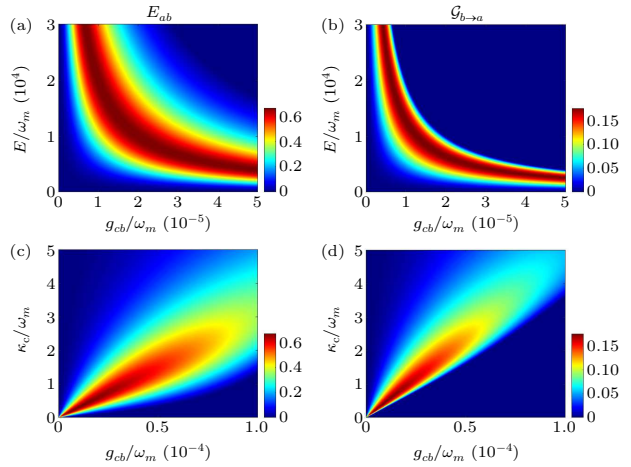


Fig. 4. (a) The steady-state entanglement E_{ab} and (b) steering $\mathcal{G}_{b\to a}$ as functions of the amplitude E of the driving laser and the photon–phonon coupling strength g_{cb}. (c) The steady-state entanglement E_{ab} and (d) steering $\mathcal{G}_{b\to a}$ as functions of the cavity dissipation rate κ_c and the photon–phonon coupling strength g_{cb}. The system parameters are the same as those in Fig. 2.

In Fig. 5, we plot the entanglement E_{ab} (a) and steering $\mathcal{G}_{b\to a}$ (b) as functions of the coefficient Λ and the thermal mean phonon number $n_{\rm th}$. Since the coefficient Λ is proportional to the Duffing nonlinearity, we can observe from Figs. 5(a) and 5(b) that the ranges of thermal mean phonon number $n_{\rm th}$ that can generate entanglement and steering first increase and then decrease as the Duffing nonlinearity increases. Notably, when Λ/ω_m reaches approximately 0.25, the system still exhibits strong entanglement even at $n_{\rm th}$ up to 10^4, suggesting robustness to thermal noise and resilience to fluctuations. However, as Λ further increases, the range of thermal noise that can sustain entanglement and steering states gradually diminishes. The entanglement nearly disappears even in the absence of thermal noise when Λ/ω_m approaches 0.5. The analysis of the observed phenomena suggests that incorporating an appropriate degree of Duffing nonlinearity can enhance the system's robustness to thermal noise and enable the system to sustain entanglement even at higher levels of thermal noise. When the mechanical resonator mode is transformed into the squeezing picture, the squeezing parameter r monotonically increases with an increase in Λ, i.e., the effective Duffing nonlinearity strength, which indicates that Λ has a positive effect on enhancing the squeezing of the mechanical resonator mode.

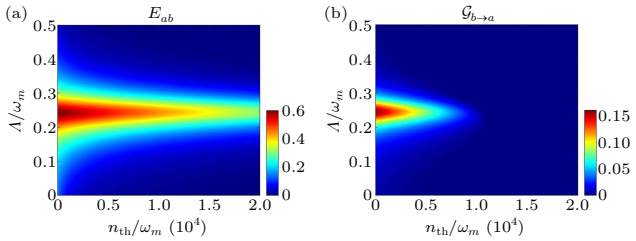


Fig. 5. (a) The steady-state entanglement E_{ab} and (b) steering $\mathcal{G}_{b\to a}$ as functions of Λ and $n_{\rm th}$. The system parameters are the same as those in Fig. 2.

Thermal noise is typically characterized by random fluctuations in position and momentum, whereas the squeezing effect of the mechanical resonator modes specifically refers to the reduction of the fluctuations in position or momentum. Therefore, in thermal noise environments, this squeezing effect essentially decreases the system's sensitivity to thermal noise, leading to an enhancement in the stability and entanglement protection of the system. However, it is crucial to note that Λ should not exceed a certain threshold. When Λ exceeds this threshold, the nonlinear effect becomes overly strong, leading to an increase in the complexity of the system's dynamical behavior and a subsequent decrease in its stability. Consequently, it will significantly narrow the range of thermal noise levels that generate entanglement and steering.

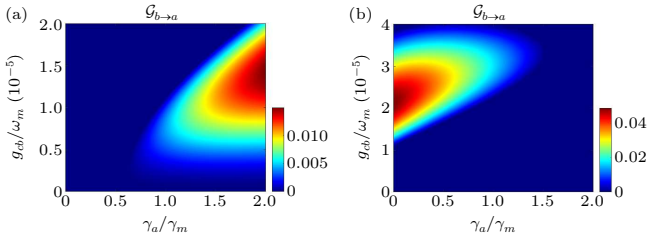


Fig. 6. (a) The steady-state steering $\mathcal{G}_{b\to a}$ and (b) steering $\mathcal{G}_{a\to b}$ as functions of the ratio of the dissipation rate of the atomic ensemble to the dissipation rate of the mechanical resonator γ_a/γ_m and the photon–phonon coupling strength g_{cb}. Here $\gamma_m/\omega_m = 0.1$ and the other parameters are the same as those in Fig. 2.

The investigation above revolves around the entanglement E_{ab} and steering $\mathcal{G}_{b\to a}$ between the atomic ensemble mode δa and the mechanical resonator mode δb, and the steering $\mathcal{G}_{a\to b}$ in the opposite direction will be added next. In Fig. 6, we plot the steering $\mathcal{G}_{b\to a}$ (a) and steering $\mathcal{G}_{a\to b}$ (b) as functions of the ratio of the dissipation rate of the atomic ensemble to the dissipation rate of the mechanical resonator γ_a/γ_m and the photon–phonon coupling strength g_{cb}. The steering $\mathcal{G}_{b\to a}$ is mainly observed when $\gamma_a > \gamma_m$, while the steering $\mathcal{G}_{a\to b}$ is primarily observed when $\gamma_m > \gamma_a$. In this regard, one can conclude that when the dissipation is different in two modes, the side with higher dissipation is more likely to be influenced by the side with lower dissipation. This is because the side with

higher dissipation is more susceptible to external perturbations and internal noise, leading to reduced stability; conversely, the side with lower dissipation maintains better stability due to a slower rate of energy loss. When the two modes interact, the side with lower dissipation is more likely to steer the side with higher dissipation due to its superior stability. However, dissipation is not optimal if it is too high. Excessive dissipation may lead to instability, energy loss and destruction of the system's state, thereby weakening the steering effect.

4. Conclusion

This paper proposes an innovative theoretical framework for achieving quantum entanglement and steering between an atomic ensemble and a mechanical resonator within a hybrid atom–optomechanical system consisting of an optical cavity, a two-level atomic ensemble and a mechanical resonator with Duffing nonlinearity. The interaction between the atomic ensemble and the mechanical resonator is facilitated through the cavity mode, which is driven by a coherent laser. Our study has demonstrated that precise tuning of the photon–phonon and collective atom–cavity coupling strengths can significantly enhance the entanglement and steering between the atomic ensemble and the mechanical resonator. Notably, the amplitude of the driving laser is crucial for optimizing the photon–phonon coupling strength, and the Duffing nonlinearity is vital for enhancing the resilience of the system to thermal noise, thereby ensuring stability and protecting the entanglement. Finally, we investigated the conditions for generating steering in different directions and found that steering always occurs from the side with lower dissipation to the side with higher dissipation. Our proposed scheme provides greater flexibility and convenience for experimental research and practical applications in quantum information processing and communication technologies.

Acknowledgments

Project supported by the National Natural Science Foundation of China (Grant No. 12204440) and Fundamental Research Program of Shanxi Province (Grant Nos. 20210302123063 and 202103021223184).

References

[1] Lanyon B P, Weinhold T J, Langford N K, Barbieri M, James D F V, Gilchrist A and White A G 2007 *Phys. Rev. Lett.* **99** 250505
[2] Einstein A, Podolsky B and Rosen N 1935 *Phys. Rev.* **47** 777
[3] Horodecki R, Horodecki P, Horodecki M and Horodecki K 2009 *Rev. Mod. Phys.* **81** 865
[4] Bennett C H, Brassard G, Crépeau C, Jozsa R, Peres A and Wootters W K 1993 *Phys. Rev. Lett.* **70** 1895
[5] Hu M J, Hu X M and Zhang Y S 2024 *Chin. Phys. Lett.* **41** 050302
[6] Li J, Zhou Y and Wang Q 2022 *Chin. Phys. Lett.* **39** 110301
[7] Vitali D, Gigan S, Ferreira A, Böhm H R, Tombesi P, Guerreiro A, Vedral V, Zeilinger A and Aspelmeyer M 2007 *Phys. Rev. Lett.* **98** 030405
[8] Barzanjeh S, Vitali D, Tombesi P and Milburn G J 2011 *Phys. Rev. A* **84** 042342
[9] Aspelmeyer M, Kippenberg T J and Marquardt F 2014 *Rev. Mod. Phys.* **86** 1391
[10] Yang Q, Hou B P and Lai D G 2017 *Opt. Express* **25** 9697
[11] Ma P C, Zhang J Q, Xiao Y, Feng M and Zhang Z M 2014 *Phys. Rev. A* **90** 043825
[12] Wu Q, Zhang J Q, Wu J H, Feng M and Zhang Z M 2015 *Opt. Express* **23** 18534
[13] Qin G Q, Yang H, Mao X, Wen J W, Wang M, Ruan D and Long G L 2020 *Opt. Express* **28** 580
[14] Shang C, Shen H Z and Yi X X 2019 *Opt. Express* **27** 25882
[15] Jiang Y J, Zhao X D, Xia S Q, Yang C J, Liu W M and Zhu Z L 2022 *Chin. Phys. Lett.* **39** 124202
[16] Xie H, Shang X, Liao C G, Chen Z H and Lin X M 2019 *Phys. Rev. A* **100** 033803
[17] Tan H, Bariani F, Li G and Meystre P 2013 *Phys. Rev. A* **88** 023817
[18] Peng R, Yang Z, Wang D and Zhou L 2023 *Opt. Express* **31** 35754
[19] Jähne K, Genes C, Hammerer K, Wallquist M, Polzik E S and Zoller P 2009 *Phys. Rev. A* **79** 063819
[20] Huang S and Chen A 2020 *Phys. Rev. A* **102** 023503
[21] Guo Y, Guo X, Li P, Shen H, Zhang J and Zhang T 2018 *Ann. Phys.* **530** 1800138
[22] Wu X J, Cheng H H, Wu Q, Bai C H and Wu S X *2024 Opt. Express* **32** 35663
[23] Li W, Li C and Song H 2016 *Phys. Rev. E* **93** 062221
[24] Genes C, Vitali D, Tombesi P, Gigan S and Aspelmeyer M 2008 *Phys. Rev. A* **77** 033804
[25] Chen X, Liu Y C, Peng P, Zhi Y and Xiao Y F 2015 *Phys. Rev. A* **92** 033841
[26] Liu Y C, Xiao Y F, Luan X, Gong Q and Wong C W 2015 *Phys. Rev. A* **91** 033818
[27] Lai D G, Huang J F, Yin X L, Hou B P, Li W, Vitali D, Nori F and Liao J Q 2020 *Phys. Rev. A* **102** 011502
[28] Zhang X Y, Zhou Y H, Guo Y Q and Yi X X 2019 *Phys. Rev. A* **100** 023807
[29] Liu J X, Yang J Y, Lu T X, Jiao Y F and Jing H 2024 *Phys. Rev. A* **109** 023519
[30] Miki D, Matsumoto N, Matsumura A, Shichijo T, Sugiyama Y, Yamamoto K and Yamamoto N 2023 *Phys. Rev. A* **107** 032410
[31] Asjad M, Tombesi P and Vitali D 2016 *Phys. Rev. A* **94** 052312
[32] Luo Y and Tan H 2020 *Quantum Sci. Technol.* **5** 045023
[33] Yang J, Lu T X, Peng M, Liu J, Jiao Y F and Jing H 2024 *Opt. Express* **32** 785
[34] Qin W, Miranowicz A, Li P B, Lü X Y, You J Q and Nori F 2018 *Phys. Rev. Lett.* **120** 093601
[35] Hu C S, Shen L T, Yang Z B, Wu H, Li Y and Zheng S B 2019 *Phys. Rev. A* **100** 043824
[36] Wei J N, Wang T, Zhang S and Wang H F 2024 *Adv. Quantum Technol.* **7** 2300374
[37] Cong L J, Luo Y X, Zheng Z G, Liu H Y, Ming Y and Yang R C 2023 *Opt. Express* **31** 34021
[38] Wu S X, Bai C H, Li G, Yu C S and Zhang T 2023 *J. Opt. Soc. Am. B* **40** 2885
[39] Luo Y X, Cong L J, Zheng Z G, Liu H Y, Ming Y and Yang R C 2023 *Opt. Express* **31** 34764
[40] Chen Y T, Du L, Zhang Y and Wu J H 2021 *Phys. Rev. A* **103** 053712
[41] Lai D G, Qin W, Hou B P, Miranowicz A and Nori F 2021 *Phys. Rev. A* **104** 043521
[42] Shi Z C, Xia Y and Song J 2013 *Quantum Inf. Process.* **12** 3179
[43] Liu Y Y, Zhang Z M, Liu J H, Wang J D and Yu Y F 2022 *Chin. Phys. B* **31** 094203
[44] Huang W J, Fang M F and Xu X 2022 *Chin. Phys. B* **31** 010301
[45] Sohail A, Hassan A, Ahmed R and Yu C S 2022 *Quantum Inf. Process.* **21** 207
[46] Sohail A, Abbas Z, Ahmed R, Shahzad A, Akhtar N and Peng J X 2023 *Ann. Phys.* **535** 2300087
[47] Liu Y, Cai Y, Xiang Y, Li F, Zhang Y and He Q 2019 *Opt. Express* **27** 33070
[48] Wu S X, Bai C H, Li G, Yu C S and Zhang T 2024 *Opt. Express* **32** 260
[49] Yang W Q, Leng X, Cheng J and Zhang W Z 2024 *Chin. Phys. B* **33** 060313
[50] Li Y, Li C, Zhang J, Dong Y and Hu H 2023 *Chin. Phys. B* **32** 044213
[51] Zhang J S and Chen A X 2020 *Opt. Express* **28** 12827

[52] Wang D Y, Bai C H, Xing Y, Liu S, Zhang S and Wang H F 2020 *Phys. Rev. A* **102** 043705
[53] Ding Z and Zhang Y 2022 *Chin. Phys. B* **31** 070304
[54] Gao X C, Wu X J, Bai C H, Wu S X and Yu C S 2023 *Opt. Express* **31** 36796
[55] Lü X Y, Liao J Q, Tian L and Nori F 2015 *Phys. Rev. A* **91** 013834
[56] Han X, Wang D Y, Bai C H, Cui W X, Zhang S and Wang H F 2019 *Phys. Rev. A* **100** 033812
[57] Zhang J S and Chen A X 2020 *Opt. Express* **28** 36620
[58] Holstein T and Primakoff H 1940 *Phys. Rev.* **58** 1098
[59] Scully M O and Zubairy M S 1997 *Quantum Optics* (Cambridge: Cambridge University Press)
[60] Vidal G and Werner R F 2002 *Phys. Rev. A* **65** 032314
[61] Kogias I, Lee A R, Ragy S and Adesso G 2015 *Phys. Rev. Lett.* **114** 060403
[62] Jacobs K and Landahl A J 2009 *Phys. Rev. Lett.* **103** 067201
[63] DeJesus E X and Kaufman C 1987 *Phys. Rev. A* **35** 5288
[64] Duan L M, Giedke G, Cirac J I and Zoller P 2000 *Phys. Rev. Lett.* **84** 2722
[65] Simon R 2000 *Phys. Rev. Lett.* **84** 2726